

## HYDROTHERMAL DECOMPOSITION OF INDUSTRIAL JAROSITE IN ALKALINE MEDIA: THE RATE DETERMINING STEP OF THE PROCESS KINETICS

A.A. González-Ibarra<sup>a,\*</sup>, F. Nava-Alonso<sup>a,b</sup>, J.C. Fuentes-Aceituno<sup>a</sup>, A. Uribe-Salas<sup>a</sup>

<sup>a</sup> CINVESTAV Unidad Saltillo, Ramos Arizpe, Mexico

<sup>b</sup> Laval University, Department of Mining, Metallurgical and Materials Engineering, Quebec, Canada

(Received 30 April 2015; accepted 25 April 2016)

### Abstract

This work examines the role of NaOH and Ca(OH)<sub>2</sub> on the hydrothermal decomposition of industrial jarosite deposited by a Mexican company in a tailings dam. The industrial jarosite is mainly composed by natrojarosite and contains 150 g Ag/t, showing a narrow particle size distribution, as revealed by XRD, fire assay, SEM-EDS and laser-diffraction analysis. The effect of the pH, when using NaOH or Ca(OH)<sub>2</sub> as alkalinizing agent was studied by carrying out decomposition experiments at different pH values and 60°C in a homogeneous size particle system (pH = 8, 9, 10 and 11) and in a heterogeneous size particle system (pH = 11). Also, the kinetic study of the process and the controlling step of the decomposition reaction when NaOH and Ca(OH)<sub>2</sub> are used was determined by fitting the data obtained to the shrinking core model for spherical particles of constant size. These results, supported by chemical (EDS), morphological (SEM) and mapping of elements (EDS) analysis of a partially reacted jarosite particle allowed to conclude that when NaOH is used, the process kinetics is controlled by the chemical reaction and when Ca(OH)<sub>2</sub> is used, the rate determining step is changed to a diffusion control through a layer of solid products.

**Keywords:** Hydrothermal decomposition; pH; Shrinking core model

### 1. Introduction

The aqueous-chemical treatment of non-ferrous metal ores and its concentrates has always been related to the separation of iron as one of its main impurities in the solution. The jarosite process was developed in the mid-sixties and represents an important purification technique to remove iron from solution at 90 – 100°C in the hydrometallurgical industry of zinc [1]. In the 1970s and 1980s, the jarosite process was improved increasing the rate of jarosite precipitation [2-4] and decreasing silver and lead coprecipitation in the jarosite precipitation and since then jarosite process has been accepted as the common process to remove iron in commercial applications.

One of the problems involved with the jarosite precipitation process is the loss of significant amounts of silver, lead, zinc and copper. Although a jarosite-type compound contain in average 200 – 300 grams of silver per ton, this cannot be recovered by direct cyanidation due to the refractory properties of this kind of compounds. Hence, jarosite should be subjected to a decomposition process to enable the recovery of the contained silver. According to Kunda

and Veltman [5] and Das et al. [1] the decomposition process may be carried out thermally or hydrothermally; the hydrothermal decomposition may proceed in acid or alkaline media. Apparently, the alkaline hydrothermal decomposition may be the most suitable pre-treatment process in order to recover the silver by cyanidation, due to the fact that both processes (i.e., decomposition and cyanidation) are carried out under similar alkaline pH value.

The decomposition of jarosite was first studied by Kunda and Veltman [5], their investigation promoted the development of three processing alternatives 1) thermal decomposition with separate recovery of hematite, ammonia and sulfur dioxide, 2) decomposition of jarosite in aqueous slurry to hematite and ammonium sulfate, or 3) decomposition in aqueous slurry to magnetite and ammonium sulfate.

In previous independent research work, Roca et al. [6] and Cruells et al. [7] studied the decomposition-cyanidation kinetics of synthetic argentojarosite in NaOH and Ca(OH)<sub>2</sub> media, and concluded that the process is controlled by chemical reaction in both media, and that the alkaline decomposition of argentojarosite presents an induction period, during which the external appearance of the jarosite

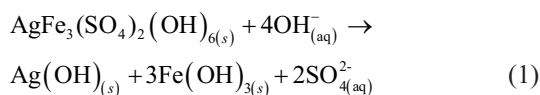
\* Corresponding author: [adrian.gonzalez@cinvestav.mx](mailto:adrian.gonzalez@cinvestav.mx)



remained unchanged and only traces of sulfate ions were found in solution.

Another important studies employing jarosite (zinc plant residue) as raw material are those conducted by Erdem et al. [8] and Turan et al. [9] in which the main goal is the recovery of lead and zinc from jarosite.

The basic principles of hydrothermal decomposition of argentojarosite in alkaline media and its effect on cyanidation have been studied by Roca et al. [6] and Viñals et al. [10], and they concluded that the alkaline decomposition of synthetic argentojarosite is characterized by the removal of sulfate ions from the lattice and the formation of a gel-type compound consisting of iron and silver hydroxides, as shown by Eq. (1).



The dissolution of sodium hydroxide or calcium hydroxide provides hydroxyl ions, which allows the formation of silver hydroxide, iron hydroxide (III) and sulfate ion in solution.

The present study objective was to determine the effect of the pH when sodium hydroxide and calcium hydroxide are used as alkalinizing agent and, to elucidate the controlling step of the decomposition process by analyzing the data obtained using the shrinking core model for spherical particles of constant size. The solid residues were also characterized chemically and morphologically, in an attempt to gain better understanding of the phenomena that control the decomposition kinetics of industrial jarosite. It is important to mention that the present study was carried out with an industrial jarosite, therefore it can be compared in terms of the rate determining step of the process kinetics obtained previously with synthetic argentojarosite [6, 7, 10-14].

## 2. Experimental

### 2.1. Materials

Industrial jarosite comes from Mexico and was obtained as a byproduct of the purification step in the hydrometallurgical process for zinc production; the most common reactants to precipitate jarosite are ammonium sulfate and sodium sulfate [1]. Therefore, natrojarosite or ammonium jarosite was expected. The sample neither was classified granulometrically nor subjected to any treatment prior to characterization.

### 2.2. Characterization

The mineralogical species were identified by X-ray diffraction (Phillips X-Pert diffractometer

equipped with a detector using Cu K $\alpha$  radiation). Gold and silver in solid samples were fire-assayed. Zn, Fe, As, Cu, Sb, S, Cd, Cr, Hg and Pb chemical analysis were carried out by atomic absorption spectroscopy (Varian SpectrAA220) and inductively coupled plasma atomic spectroscopy (Perkin Elmer Optima 8300). The  $d_{80}$  of the size fractions was estimated from the particle size distribution measured with laser diffraction particle size analyzer (Coulter LS-100Q). Selected samples were characterized by scanning electron microscopy (Philips XL30-ESEM) in conjunction with energy dispersive spectrometry (EDAX Genesis).

### 2.3. Decomposition tests

All the decomposition experiments were performed in an agitated batch reactor (500 mL glass baker), magnetically stirred at 350 rpm. The reactor was provided with a pH electrode (Cole-Parmer) and a temperature probe. The general procedure for the decomposition experiments was as follows: 500 mL of deionized water and alkalinizing agent in solution were poured in the reactor. After adjusting the pH (to 8, 9, 10 and 11) and the temperature at 60 °C (according to not reported preliminary test and statistical analysis 60 °C is the best temperature to decompose industrial jarosite), 0.5 g of industrial jarosite were placed in the reactor while stirring. The temperature was maintained constant as well as the pH (adding NaOH or Ca(OH)<sub>2</sub> in solution) during the test and all solutions were prepared with reagent grade chemicals and deionized water. Samples of the solution were withdrawn at predetermined times during the decomposition period for analysis of sulfate by turbidimetry (La Motte 2020) in order to follow the decomposition process of jarosite as % of decomposition. Additional experiments were performed in order to obtain solid samples of partially decomposed jarosite; the samples were filtered and left to air dry. One sample corresponds to a partially decomposed jarosite using NaOH as alkalinizing agent; this was characterized by scanning electron microscopy (Philips XL30-ESEM) in conjunction with energy dispersive spectrometry (EDAX Genesis). The characterization of the samples of partially decomposed jarosite using Ca(OH)<sub>2</sub> as alkalinizing agent was complemented with chemical and morphological characterization and mapping of elements by scanning electron microscopy and energy dispersive spectrometry since the results observed appear to be at odds with the results obtained for synthetic argentojarosite [6, 7, 11-14].

### 2.4. Kinetic study and the shrinking core model

Decomposition tests were carried out in order to



determine the different rate determining steps of the process kinetics when NaOH or Ca(OH)<sub>2</sub> are used as alkalinizing agent.

In order to determine the controlling step of the decomposition process, the hydrothermal decomposition experiments were analyzed with the shrinking core model. Equation (2) is proposed for a process whose kinetics is controlled by the chemical reaction [15].

$$t(bk_s C_A / R_p \rho_B) = 1 - (1 - X)^{1/3} \quad (2)$$

Where:

t = reaction time (s)

b = reaction stoichiometric coefficient

k<sub>s</sub> = rate constant of the surface reaction (m/s)

C<sub>A</sub> = concentration of the reactant aqueous species (mol/m<sup>3</sup>)

R<sub>p</sub> = particle radius (m)

ρ<sub>B</sub> = molar density of the industrial jarosite in the solid sample (mol/m<sup>3</sup>)

X = fractional conversion (decomposition) of the jarosite

Equation (3) is the model's equation that governs the process whose kinetics is controlled by the diffusion of the aqueous species through the porous layer of products [8].

$$t(6bD_e C_{Al} / R_p^2 \rho_B) = 1 - 3(1 - X)^{2/3} + 2(1 - X) \quad (3)$$

Where:

D<sub>e</sub> = effective diffusion coefficient of the aqueous species through the porous layer (m<sup>2</sup>/s)

Equations (1) and (2) are valid for systems in which the particle size is homogeneous and not for a sample containing an ore size distribution. The industrial jarosite used in this study consist of a particle size distribution and therefore, the kinetic study was carried out considering a multi-size particle

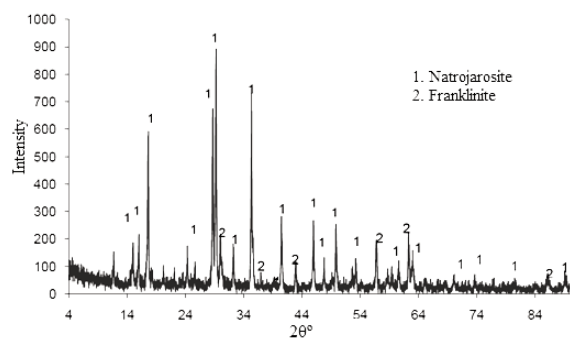


**Figure 1.** XRD pattern of the industrial jarosite sample. The XRD pattern was acquired on a x-ray diffractometer equipped with a detector using Cu Kα radiation.

**Table 1.** Chemical composition of the industrial jarosite.

| Fire assay | Element   | Au   | Ag  | AAS | Element | Zn   | Fe    | As    | Cu    | Sb    | Cd    | Cr    | Hg      | Pb   | Mg, Si, Al, K and Na |
|------------|-----------|------|-----|-----|---------|------|-------|-------|-------|-------|-------|-------|---------|------|----------------------|
|            | Grade g/t | 0.03 | 156 |     | wt. %   | 4.48 | 45.94 | 0.012 | 0.756 | 0.002 | 0.188 | 0.005 | <0.0001 | 0.95 | 47.667               |

system at pH = 11 only, since the main objective of this work is to determine the controlling step of the hydrothermal decomposition process. It is necessary to define a constant “a (μm/min)” as bC<sub>A</sub>K<sub>s</sub>/ρ<sub>B</sub> to obtain Eq. (4) for a process whose controlling step is the chemical reaction and 6bCD<sub>e</sub>/ρ<sub>B</sub> to obtain Eq. (5) for a process whose controlling step is diffusion of the aqueous species through the porous layer of reaction products.

$$at/R_p = 1 - (1 - X)^{1/3} \quad (4)$$

$$at/R_p^2 = 1 - 3(1 - X)^{2/3} + 2(1 - X) \quad (5)$$

### 3. Results and discussion

#### 3.1. Characterization of the jarosite sample

The detailed chemical composition of the jarosite sample is shown in Table 1.

The silver is the main valuable element in the industrial jarosite (156 g/t). Other elements that may be of economic interest are zinc, iron and copper. The presence of elements that may pose environmental issues, such as Hg, Cd and As, were also observed and at this respect studies have been made by Özverdi and Erdem [16] since this kind of residues are considered as hazardous waste due to their heavy metal content [17].

Figure 1 presents the diffractogram of industrial jarosite, clearly showing the presence of natrojarosite (peak 1) and franklinite (peak 2). The natrojarosite or sodium jarosite is a species that corresponds to a jarosite-type compound, and their presence indicates that sodium sulfate was added in the purification step of the hydrometallurgical process to obtain zinc. The sample was also characterized by SEM and EDS. Figure 2a shows the morphology of the agglomerates that form the industrial jarosite. EDS analysis (see Fig. 2b) revealed the presence of Ca (0.19 wt. %), O (52.20 wt. %), Mg (0.31 wt. %), Si (4.87 wt. %), S (11.11 wt. %), Pb (4.65 wt. %), Fe (22.29 wt. %), Cu (0.75 wt. %) and Zn (2.47 wt. %). The chemical composition and the EDS pattern were useful to validate the conclusions obtained by the data fitted to the mathematical model (see Ca content). The particle size distribution of the jarosite sample was characterized by laser diffraction. The jarosite (Fig. 3) shows a narrow size distribution of fine particles with a d<sub>80</sub> = 24 μm (Fig. 4).

It is well known that when ores are treated, the size reduction processes are one of the most expensive stages in the mining-metallurgical industry. A byproduct with narrow size distribution and a fine size (d<sub>80</sub> = 24 μm) is very attractive in terms of the recovery of silver and other valuable metals contained in it.



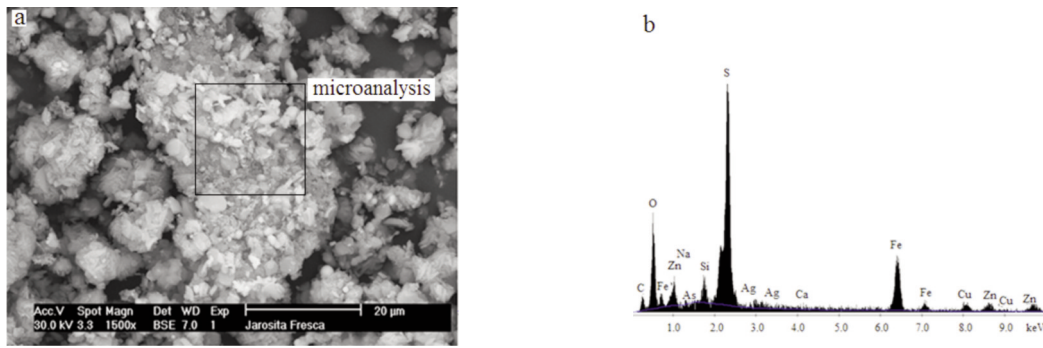


Figure 2. SEM micrograph and EDS spectrum of the industrial jarosite sample.

### 3.2. Kinetics and controlling step of the industrial jarosite decomposition: NaOH as alkalinizing agent

As mentioned in the experimental section, hydrothermal decomposition experiments at different pH values (8, 9, 10 and 11) were carried out. Figure 5 presents the effect of four different pH values on the jarosite decomposition kinetics at 60°C. It is observed that at pH = 11 the decomposition is completed in about three minutes, at pH = 10 the decomposition is 81 % after 15 minutes and at pH 9 or 8 the decomposition is relatively small after 15 minutes (37 % and 24 %, respectively). This difference in the process kinetics can be related to the different concentration of hydroxide ions present in each experiment, i. e., the

experiment carried out at pH 11 had a higher OH<sup>-</sup> concentration than the systems performed at pH 10, 9 and 8, respectively. Actually, as shown in Eq. (1), hydroxide ions are necessary in order to promote the jarosite decomposition, and according to the kinetic theory of chemical reactions, an increase of the reactants concentration, in this case OH<sup>-</sup> ions enhances the jarosite decomposition kinetics.

Figure 6 shows the experimental data of Fig. 5 fitted to Eq. (2) for the jarosite decomposition in solutions of pH 8, 9, 10 and 11 adjusted with NaOH. It is observed that the hydrothermal decomposition kinetics is most probably controlled by the chemical reaction, as reflected by the fairly high correlation coefficients obtained and by the activation energy of 40.6 kJmol<sup>-1</sup> determined by the authors in an unpublished work. According to this, the course of reaction is not affected by the presence of a layer of products (Ag(OH) and Fe(OH)<sub>3</sub>, according to Eq. (1)), either because this does not grow onto the unreacted core surface or because it is highly porous. It is worth noting that in Eq. (2) the term  $1-(1-X)^{1/3}$  represents the fraction of time required to fully complete the decomposition reaction. The amount of reacting material at any time is proportional to the available surface of the unreacted core.

A solid sample of partially decomposed jarosite was characterized by SEM and EDS (Fig. 7). Figure

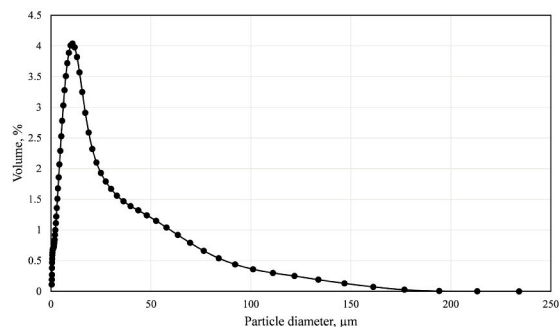


Figure 3. Particle size distribution of the industrial jarosite sample.

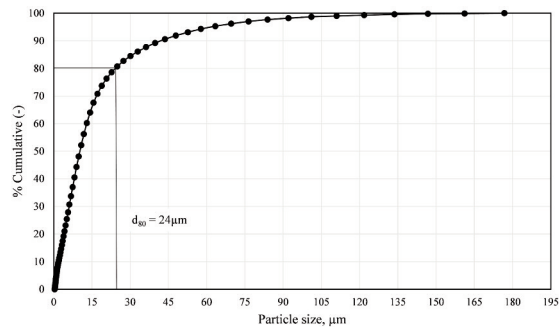


Figure 4. Cumulative undersize plot of the industrial jarosite sample.

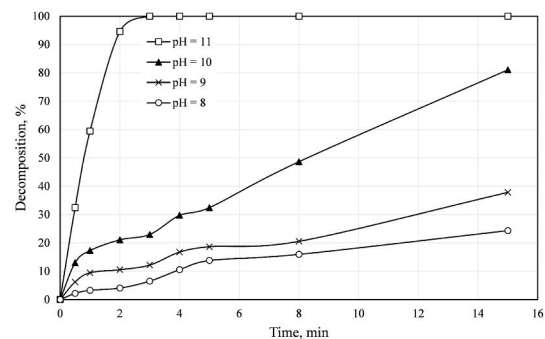
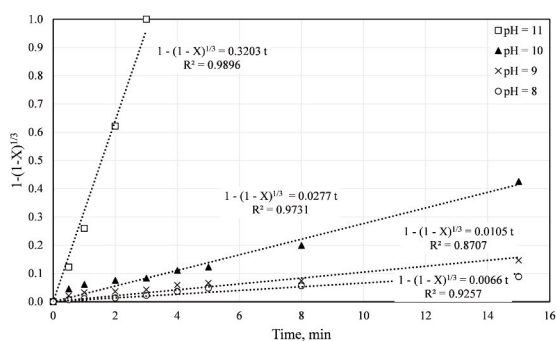


Figure 5. Effect of pH on the kinetics of the industrial jarosite hydrothermal decomposition (0.5 g of industrial jarosite, 500 mL of deionized water at 60°C and NaOH as alkalinizing agent).



**Figure 6.** Kinetic decomposition data of the industrial jarosite fitted to the chemical reaction control equation of the shrinking core model for spherical particles (0.5 g of industrial jarosite, 500 mL of deionized water at 60°C and NaOH as alkalinizing agent).

7a shows the morphology of a typical aggregate of jarosite particles at 40 % of decomposition. The EDS analysis (Fig. 7b) revealed the presence of Ca (0.76 wt. %), O(39.16 wt. %), Mg(0.31 wt. %), Si(3.88 wt. %), S(9.33 wt. %), Pb(3.30 wt. %), Fe(35.11 wt. %), Cu(1.04 wt. %) and Zn(6.28 wt. %). These numbers indicate that the jarosite partially decomposed with sodium hydroxide shows a chemical composition similar to that of the unreacted jarosite. However, it is interesting to observe the content of oxygen and sulfur in Fig. 7 and Fig. 2, i. e., the wt % is higher in Fig. 2 than in Fig. 7, revealing that the jarosite was partially decomposed in Fig 2; it is important to remember that according to Eq. (1) sulfate ions are produced from the jarosite decomposition, therefore it was expected that the content of oxygen and sulfur in the solid residue of Fig. 2 would decrease.

Furthermore, comparing the micrographs shown in Fig. 2a and Fig. 7a, it is interesting to observe a decrease in the jarosite particle size, suggesting that as the decomposition proceeds the jarosite particle is contracted.

Industrial jarosite used for the study of alkaline decomposition consists of particles of various sizes, therefore the kinetic study was also carried out on a multi-size particle system adjusting the size

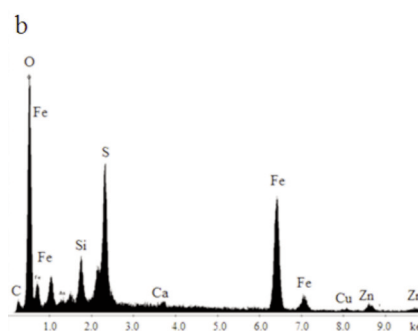
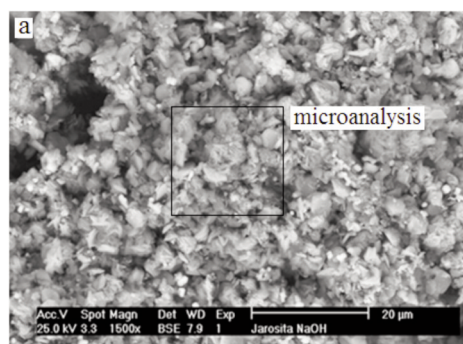


**Figure 7.** SEM micrograph and EDS spectrum of industrial jarosite partially decomposed (40 % decomposed adding NaOH to adjust pH at 11).

distribution data of Fig. 4 to Eq. 4 and trying different values for constant “a” to obtain the minimum value of optimization factor (F.O.). It is observed in Table 2 that the reaction of particles of 2.36 μm diameter occurs completely after 0.5 minutes and after 15 minutes the decomposition of all the size classes of the industrial jarosite is completed. Obviously, smaller particles react faster than coarser ones and initially contribute more to the global decomposition.

### 3.3. Kinetics and controlling step of the industrial jarosite decomposition: $\text{Ca}(\text{OH})_2$ as alkalinizing agent

Experiments at different pH values (8, 9, 10 and 11) adjusted with  $\text{Ca}(\text{OH})_2$  were carried out. Figure 8 presents the experimental results obtained showing the effect of pH on the jarosite decomposition kinetics at 60°C, where it is observed that at pH 11 the decomposition reaches 81 % at 40 minutes, and that at pH 10 the decomposition is practically the same. Interestingly, when the pH was adjusted at 8 or 9 the jarosite decomposition was relatively small (ca. 35 and 50%, respectively).

Figure 9 shows the experimental data of these test fitted to the equation for processes governed by diffusion, Eq. (3); The fair fitting to this equation suggests that the decomposition of jarosite when

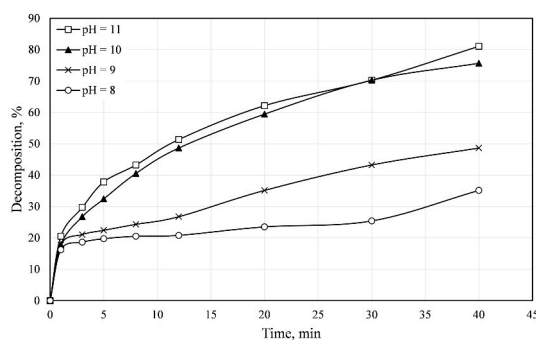


**Figure 8.** Effect of pH on the kinetics of the industrial jarosite hydrothermal decomposition (0.5 g of industrial jarosite, 500 mL of deionized water at 60°C and  $\text{Ca}(\text{OH})_2$  as alkalinizing agent).

**Table 2.** Jarosite volume fraction converted at pH = 11 when sodium hydroxide is used as alkalinizing agent;  $a = 3.288 \mu\text{m}/\text{min}$  (Eq. (4)).

| Diameter, $\mu\text{m}$                | Vol. Fraction | Time, min |       |       |       |       |       |       |       |       |
|--|---------------|-----------|-------|-------|-------|-------|-------|-------|-------|-------|
|  |               | 0         | 0.5   | 1     | 2     | 3     | 4     | 5     | 8     | 15    |
| 2.36                                   | 0.254         | 0.000     | 0.247 | 0.254 | 0.254 | 0.254 | 0.254 | 0.254 | 0.254 | 0.254 |
| 7.94                                   | 0.268         | 0.000     | 0.134 | 0.214 | 0.267 | 0.268 | 0.268 | 0.268 | 0.268 | 0.268 |
| 13.21                                  | 0.154         | 0.000     | 0.051 | 0.089 | 0.134 | 0.151 | 0.154 | 0.154 | 0.154 | 0.154 |
| 18.17                                  | 0.087         | 0.000     | 0.022 | 0.039 | 0.064 | 0.079 | 0.085 | 0.087 | 0.087 | 0.087 |
| 22.82                                  | 0.044         | 0.000     | 0.009 | 0.016 | 0.028 | 0.036 | 0.041 | 0.043 | 0.044 | 0.044 |
| 30.59                                  | 0.070         | 0.000     | 0.011 | 0.020 | 0.036 | 0.048 | 0.057 | 0.063 | 0.070 | 0.070 |
| 42.08                                  | 0.042         | 0.000     | 0.005 | 0.009 | 0.017 | 0.023 | 0.028 | 0.033 | 0.040 | 0.042 |
| 52.85                                  | 0.024         | 0.000     | 0.002 | 0.004 | 0.008 | 0.011 | 0.014 | 0.016 | 0.021 | 0.024 |
| 67.1                                   | 0.027         | 0.000     | 0.002 | 0.004 | 0.007 | 0.010 | 0.013 | 0.015 | 0.021 | 0.026 |
| 88.76                                  | 0.017         | 0.000     | 0.001 | 0.002 | 0.004 | 0.005 | 0.006 | 0.008 | 0.011 | 0.016 |
| 111.45                                 | 0.006         | 0.000     | 0.000 | 0.001 | 0.001 | 0.001 | 0.002 | 0.002 | 0.003 | 0.005 |
| 134.3                                  | 0.005         | 0.000     | 0.000 | 0.000 | 0.001 | 0.001 | 0.001 | 0.002 | 0.002 | 0.004 |
| 161.8                                  | 0.002         | 0.000     | 0.000 | 0.000 | 0.000 | 0.000 | 0.000 | 0.001 | 0.001 | 0.001 |
| $X_{\text{calculated}} =$              |               | 0.000     | 0.483 | 0.653 | 0.821 | 0.889 | 0.924 | 0.945 | 0.976 | 0.995 |
| $X_{\text{experimental}} =$            |               | 0.000     | 0.324 | 0.595 | 0.946 | 1.000 | 1.000 | 1.000 | 1.000 | 1.000 |
| $(X_{\text{exp}} - X_{\text{calc}})^2$ |               | 0.000     | 0.025 | 0.003 | 0.016 | 0.012 | 0.006 | 0.003 | 0.001 | 0.000 |
| F.O. =                                 |               |           |       |       |       |       |       |       |       | 0.066 |

$\text{Ca}(\text{OH})_2$  is used as alkalinizing agent, is a process controlled by the diffusion of aqueous species through a porous layer of products. It is worth mentioning that the last result is also supported by the value of activation energy determined which corresponds to  $19.56 \text{ kJmol}^{-1}$  (unpublished work by the authors).

The term  $1-3(1-X)^{2/3}+2(1-X)$  represents the fraction of time required to fully complete the decomposition reaction.

A sample of partially decomposed jarosite was

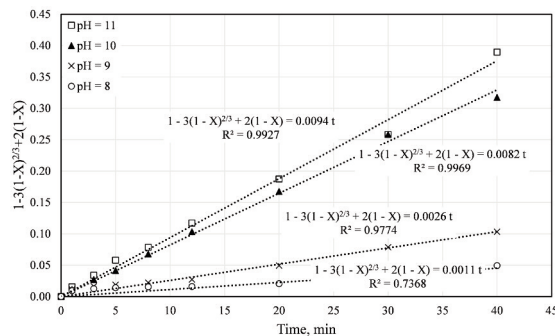


**Figure 9.** Kinetic decomposition data of the industrial jarosite fitted to the diffusion control equation of the shrinking core model for spherical particles (0.5 g of industrial jarosite, 500 mL of deionized water at  $60^\circ\text{C}$  and  $\text{Ca}(\text{OH})_2$  as alkalinizing agent).

characterized by SEM and EDS (Fig. 10). Figure 10a shows the typical morphology of jarosite particles aggregate at 48 % decomposition. The EDS analysis (see Fig. 10b) revealed the presence of Ca(9.42 wt. %), O(49.22 wt. %), Mg(0.42 wt. %), Si(3.95 wt. %), S(7.25 wt. %), Pb(2.19 wt. %), Fe(21.22 wt. %), Cu(0.64 wt. %) and Zn(4.94 wt. %). The content of oxygen and sulfur is lower than of the fresh jarosite (Fig. 2), showing that the jarosite was partially decomposed releasing ions into the bulk solution.

According to the EDS spectrum of the chemical analysis shown in Fig. 10b, an important amount of calcium appears on the surface of the partially decomposed jarosite adding  $\text{Ca}(\text{OH})_2$  to adjust pH. Actually, there is larger amount of calcium (ca. 9.4%), compared to that measured in the surface of partially decomposed jarosite adding NaOH to adjust pH (0.76%).

In this case, the diffusion of the hydroxyl ion through the layer of products to reach the unreacted core or the diffusion of the  $\text{SO}_4^{2-}$  ions in the opposite direction (e.g., Eq. (1)), is the phenomena that control the decomposition process. It can be observed in the SEM micrograph and mapping of location elements (Ca and Fe) of Fig. 11, that the product layer coating the particle of the partially decomposed jarosite using calcium hydroxide as alkalinizing agent is a calcium-iron compound.

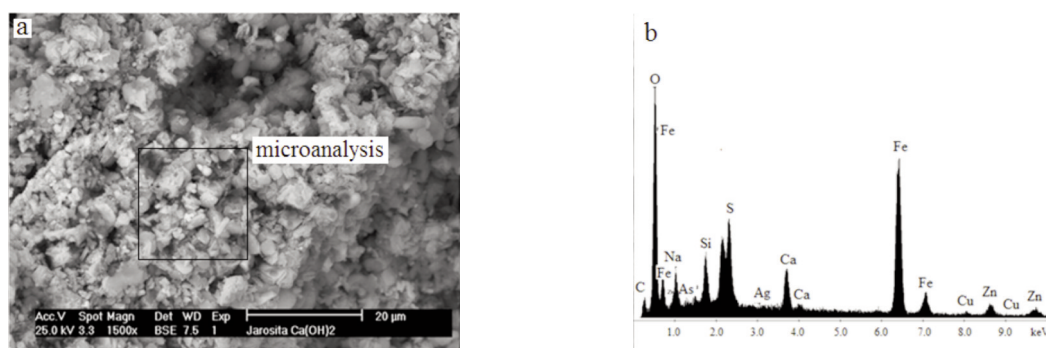


Figure 10. SEM micrograph and EDS spectrum of the industrial jarosite partially decomposed (48 % decomposed adding Ca(OH)<sub>2</sub> to adjust pH at 11).

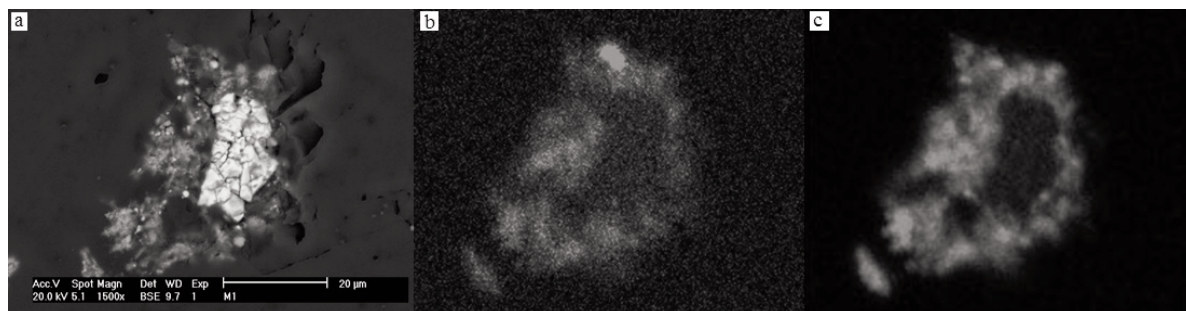


Figure 11. SEM micrograph (a) and mapping of location elements for Ca (b) and Fe (c). Jarosite decomposed at 85 % using Ca(OH)<sub>2</sub> as alkalinizing agent.

Table 3. Jarosite volume fraction converted at pH = 11 when calcium hydroxide is used as alkalinizing agent; a = 0.88 μm/min (Eq. (5)).

| Diameter, μm                | Vol. Fraction | Time, min |       |       |       |       |        |        |        |        |       |
|-----------------------------|---------------|-----------|-------|-------|-------|-------|--------|--------|--------|--------|-------|
|                             |               | 0.000     | 1.000 | 3.000 | 5.000 | 8.000 | 12.000 | 20.000 | 30.000 | 40.000 |       |
| 2.36                        | 0.254         | 0.000     | 0.148 | 0.219 | 0.254 | 0.254 | 0.254  | 0.254  | 0.254  | 0.254  |       |
| 7.94                        | 0.268         | 0.000     | 0.052 | 0.087 | 0.110 | 0.135 | 0.159  | 0.194  | 0.222  | 0.268  |       |
| 13.21                       | 0.154         | 0.000     | 0.018 | 0.031 | 0.040 | 0.049 | 0.059  | 0.074  | 0.088  | 0.098  |       |
| 18.17                       | 0.087         | 0.000     | 0.008 | 0.013 | 0.017 | 0.021 | 0.025  | 0.032  | 0.038  | 0.043  |       |
| 22.82                       | 0.044         | 0.000     | 0.003 | 0.005 | 0.007 | 0.008 | 0.010  | 0.013  | 0.016  | 0.018  |       |
| 30.59                       | 0.07          | 0.000     | 0.004 | 0.006 | 0.008 | 0.010 | 0.012  | 0.016  | 0.019  | 0.022  |       |
| 42.08                       | 0.042         | 0.000     | 0.002 | 0.003 | 0.004 | 0.004 | 0.005  | 0.007  | 0.008  | 0.010  |       |
| 52.85                       | 0.024         | 0.000     | 0.001 | 0.001 | 0.002 | 0.002 | 0.002  | 0.003  | 0.004  | 0.004  |       |
| 67.1                        | 0.027         | 0.000     | 0.001 | 0.001 | 0.001 | 0.002 | 0.002  | 0.003  | 0.003  | 0.004  |       |
| 88.76                       | 0.017         | 0.000     | 0.000 | 0.001 | 0.001 | 0.001 | 0.001  | 0.001  | 0.002  | 0.002  |       |
| 111.45                      | 0.006         | 0.000     | 0.000 | 0.000 | 0.000 | 0.000 | 0.000  | 0.000  | 0.000  | 0.001  |       |
| 134.3                       | 0.005         | 0.000     | 0.000 | 0.000 | 0.000 | 0.000 | 0.000  | 0.000  | 0.000  | 0.000  |       |
| 161.8                       | 0.002         | 0.000     | 0.000 | 0.000 | 0.000 | 0.000 | 0.000  | 0.000  | 0.000  | 0.000  |       |
| X <sub>calculated</sub> =   |               | 0.000     | 0.236 | 0.368 | 0.443 | 0.487 | 0.532  | 0.597  | 0.655  | 0.724  |       |
| X <sub>experimental</sub> = |               | 0.000     | 0.205 | 0.297 | 0.378 | 0.432 | 0.514  | 0.622  | 0.703  | 0.811  |       |
| (exp - calc) <sup>2</sup>   |               | 0.000     | 0.001 | 0.005 | 0.004 | 0.003 | 0.000  | 0.001  | 0.002  | 0.008  |       |
| FO =                        |               |           |       |       |       |       |        |        |        |        | 0.024 |



This calcium-iron compound that coated the jarosite particles hinders the direct contact between the hydroxyl ions and the unreacted core and the rapid diffusion of the  $\text{SO}_4^{2-}$  ion towards the bulk solution. According to the chemical analysis spectrum of Fig. 10, the weight ratio Fe/Ca of partially reacted jarosite is 2.25, which is similar to that of calcium ferrite ( $\text{CaFe}_2\text{O}_4$ ) (2.8); thus suggesting calcium-iron compound may be the responsible of the more compacted (or less porous) product layer observed, via the precipitation of a calcium ferrite-type compound.

If the hydrothermal decomposition process is controlled by chemical reaction (when NaOH is added), the jarosite decomposition is expected to occur faster due to either the absence of a porous layer of products on the surface or to the development of a highly porous layer; the presence of a compact layer of products, as observed when  $\text{Ca}(\text{OH})_2$  is added, would indeed hinder the jarosite decomposition.

The decomposition process in  $\text{Ca}(\text{OH})_2$  media, at odds with conclusions of previous studies [6, 7, 11-13], is controlled by diffusion of the aqueous species through the porous layer of products.

Industrial jarosite used for the study of alkaline decomposition is constituted by particles of various sizes; kinetic study was also carried out on a multi-size particle system adjusting the size distribution data of Fig. 4 to Eq. 5 and trying different values for constant "a" to obtain the minimum value of optimization factor (F.O.). It is observed in Table 3 that the reaction of particles below 2.36  $\mu\text{m}$  of diameter occurs completely in three minutes; any other fraction size got its complete reaction after 40 minutes.

#### 4. Conclusions

In the present study, the hydrothermal decomposition of industrial jarosite using NaOH and  $\text{Ca}(\text{OH})_2$  as alkalinizing agent was investigated in order to determine the controlling step of the process kinetics by taking in consideration the effect of pH in a homogeneous size particle system (pH = 8, 9, 10 and 11) and in a heterogeneous size particle system (pH = 11). The data obtained were analyzed using the shrinking core model for spherical particles of constant and variable size. On the basis of these results the following conclusions can be drawn:

1. The industrial jarosite stored in a tailings dam of a Mexican metallurgical plant corresponds mainly to natrojarosite with a silver content of 156 g/t and  $d_{80} = 24 \mu\text{m}$ .

2. The experimental data obtained indicate that the pH has a significant effect on the hydrothermal decomposition when either NaOH or  $\text{Ca}(\text{OH})_2$  is added to control pH.

3. The total hydrothermal decomposition of the industrial jarosite is completed in three minutes when

NaOH is added to adjust the pH at 11.

4. The total hydrothermal decomposition of the industrial jarosite is completed after 40 minutes when  $\text{Ca}(\text{OH})_2$  is added to adjust the pH at 11.

5. The hydrothermal decomposition process adding NaOH as alkalinizing agent is controlled by chemical reaction, therefore, the reaction kinetics is independent of the presence of any layer of products. The amount of reacting material is proportional to the available surface of the unreacted core. The hydroxyl ions react directly with the jarosite unreacted core.

6. The hydrothermal decomposition process adding  $\text{Ca}(\text{OH})_2$  as alkalinizing agent is controlled by diffusion. The jarosite particles were coated by a product layer that slows down the reaction of the hydroxyl ions with the jarosite unreacted core.

7. Calcium is the responsible of the more compacted product layer observed, via the precipitation of a calcium ferrite-type compound.

#### Acknowledgments

The authors are grateful to CONACYT (Mexico) for the postgraduate scholarship awarded to A. A. González-Ibarra, and for the research project CB2010/153885.

#### References

- [1] G. K. Das, S. Acharya, S. Anand, R. P. Das, *Miner. Process. Extr. Metall. Rev.*, 16 (1996) 185-210.
- [2] V. Arregui, A. R. Gordon, G. Steinveit, In TMS-AIME'80: lead-tin-zinc, J. M. Cigan, T. S. Mackey, T. J. O'Keefe (Eds.), New York, 1979, p. 97-123.
- [3] J. E. Dutrizac, *Metall. Trans. B* 14B (1983) 531-539.
- [4] J. E. Dutrizac, *Hydrometallurgy*, 42 (1996) 293-312
- [5] W. Kunda, H. Veltman, *Metall. Trans. B*, 10 (1979) 439-446.
- [6] A. Roca, F. Patiño, J. Viñals, C. Nuñez, *Hydrometallurgy*, 33 (1993) 341-357.
- [7] M. Cruells, A. Roca, F. Patiño, E. Salinas, I. Rivera, *Hydrometallurgy*, 55 (2000) 153-163.
- [8] M. Erdem, M. Yurten, *J. Min. Metall. Sect. B-Metall.* 51 (1) B (2015) 89-95.
- [9] M. D. Turan, H. S. Altundogan, F. Tümen, *Hydrometallurgy*, 75 (1-4) (2004) 169-176.
- [10] J. Viñals, A. Roca, M. Cruells, C. Nuñez, In EMC'91: non-ferrous metallurgy-present and future, Elsevier, London, 1991, p. 11-17.
- [11] F. Patiño, J. Viñals, A. Roca, C. Nuñez, *Hydrometallurgy*, 34 (1994) 279-291.
- [12] F. Patiño, D. Cordoba, M. Yta, *J. Mex. Chem. Soc.* 40 (1996) 61-64.
- [13] F. Patiño, E. Salinas, M. Cruells, A. Roca, *Hydrometallurgy*, 49 (1998) 323-336.
- [14] F. Patiño, M. Cruells, A. Roca, M. Pérez, *Hydrometallurgy*, 70 (2003) 153-161.
- [15] O. Levenspiel, *Chemical Reaction Engineering*, John Wiley&Sons, New York, 1999, p. 357.
- [16] A. Özverdi, M. Erdem, *Hydrometallurgy*, 100 (2010) 103-109.
- [17] H. S. Altundogan, M. Erdem, R. Orhan, F. Tumen, *Tr. J. Eng. Environ.* 22 (1998) 167-177.

